

# Reduced-order modelling of the Reynolds equation for flexible structures

A.Missoffe<sup>\*</sup>, J.Juillard<sup>\*</sup> and D.Aubry<sup>\*\*</sup>

<sup>\*</sup>SUPELEC, Dpt. of Measurement, 3 rue Joliot-Curie, 91192 Gif-sur-Yvette, FRANCE, alexia.missoffe@supelec.fr, jerome.juillard@supelec.fr

<sup>\*\*</sup>LMSS-MAT, ECP, CNRS UMR 8579, Grande Voie des Vignes, 92295 Châtenay-Malabry Cedex, FRANCE, denis.aubry@ecp.fr

## ABSTRACT

In MEMS devices, the behaviour of a fluid in small gaps between structures moving perpendicularly to each other is referred to as squeezed-film damping. This paper presents a reduced model of the non-linear Reynolds equation for a flexible structure using a modal representation, the only hypothesis made being small pressure variations. A change of variables is used so that the spatial differential operator appearing in the transformed Reynolds equation is the Laplacian, the eigenmodes of which are very simple to compute. This results in reduced construction costs compared to POD (Proper Orthogonal Decomposition) modes, for example. We first present this model with respect to the existing work. The derivation of the reduced model is then given and the approach is validated by comparing the results to those obtained with a finite difference model.

**Keywords:** squeezed-film damping, amplitude effects, reduced-order model, modal representation.

## 1 INTRODUCTION

Correct modelling of damping is essential to capture the dynamic behaviour of a MEMS device. Our interest is squeeze-film damping which models the behaviour of a fluid in small gaps between a fixed surface and a structure moving perpendicular to this surface (Fig.1). The lateral dimensions of the surfaces are large compared to the gap and the system is considered isothermal. Squeeze film damping is then governed by the Reynolds equation [1]:

$$\nabla(G^{-3}P\nabla P) = 12\mu \frac{\partial GP}{\partial t}, \quad (1)$$

where  $G(x,y,t)$  is the distance between the moving and fixed surface,  $P(x,y,t)$  is the pressure and  $\mu$  is the viscosity of the fluid. This equation is nonlinear and it is often coupled to the equation governing the mechanical behaviour of the structure. For small excitation frequencies or amplitudes it behaves as a nonlinear damper. For larger amplitudes or frequencies, the gas has no time to flow away and the pressure builds up creating a stiffening effect coupled to the damping effect.

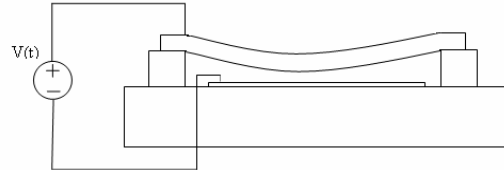


Fig. 1 - Schematic drawing of a microswitch. When a voltage is applied to the beam, the electrostatic forces cause the structure to pull-in. Damping, which influences the switching time, plays a key role in such devices.

Most existing reduced-order models of the Reynolds equation solve the linearized Reynolds equation based on the hypothesis of small pressure variations, rigidity of the moving plate [2] or/and of small displacements [3,4,5]:

$$\nabla^2 p - \frac{12\mu}{G_0^2 P_0} \frac{\partial p}{\partial t} = \frac{12\mu}{G_0^3} \frac{\partial G}{\partial t}, \quad (2)$$

where  $G_0$  is the gap corresponding to the operating point,  $P_0$  the ambient pressure, and  $p$  the pressure variation.

In [4], Younis solves the nonlinear Euler-Bernoulli beam equation to determine an initial deformation and then linearizes the dynamic von Karman plate equations and the compressible Reynolds equation near this operating point. In [3] and [5], the authors consider flexible structures and use a modal projection method, the modes being the mechanical modes, to extract modal frequency-dependent damping and stiffening coefficients for a determined operating point. The Reynolds equation is integrated in the final model via these coefficients. To extend the case to large displacements, Mehner [5] gives an expression of these coefficients as a function of mechanical modal coordinates established by fitting of simulation data at different initial deformations.

In the present paper, the nonlinear Reynolds equation is projected on pressure mode shapes, as in [6] and [7]. The approaches presented in [6] and [7] are valid for flexible structures with large displacements and large pressure variations. This is in contrast with our approach which is also valid for large displacements and flexible structures but assumes small pressure variations. However, it is much less costly to establish a reduced-order model for the squeezed-film with our method than with those presented in [6] and [7]. In [6], Hung and al. extract mode shapes from simulation data via proper orthogonal decomposition,

which requires a heavy complete finite element simulation. In [7], Rewiński and al. construct a projection base by concatenation of Krylov bases extracted from finite difference models linearized around different operating points chosen along a training trajectory. Our technique is based on a transformation of (1) through a change of variables so that the spatial differential operator does not depend on time, assuming small pressure variations. The transformed equation involves only the Laplacian, the eigenmodes of which are used. This is an advantage compared to the heavy construction cost implied by either the complexity of the finite element simulations [6], the number of them [5] or the necessity of a training trajectory [7].

In the next section, we show how the Reynolds equation may be transformed into an equation with a time-independent spatial differential operator. The resulting reduced-order model is then compared to a finite-difference model of the Reynolds equation.

## 2 PRINCIPLE

### 2.1 Transformation of the Reynolds equation

Let us consider a fixed two-dimensional domain  $\Omega$ , with border  $\partial\Omega$ , spatial coordinates  $x$  and  $y$  and time coordinate  $t$ . In the case of small pressure variations, the Reynolds equation on that domain is:

$$\frac{\partial}{\partial x} \left( G^3 \frac{\partial p}{\partial x} \right) + \frac{\partial}{\partial y} \left( G^3 \frac{\partial p}{\partial y} \right) = 12\mu \left( \frac{\partial G}{\partial t} + \frac{1}{P_0} \frac{\partial G p}{\partial t} \right), \quad (3)$$

where  $\mu$  is the fluid viscosity,  $P_0$  is the ambient pressure,  $G$  is the distance between the flexible structure and the substrate and  $p$  is the pressure variation. The boundary conditions for (3) are usually chosen as:

$$p(M) = 0, M \in \partial\Omega. \quad (4)$$

In order to solve (3) for the pressure variation, one first transforms it in the following way. Let us assume:

$$p(x, y, t) = G^{-3/2} \varphi(x, y, t). \quad (5)$$

Equation (3) then becomes:

$$G^{3/2} \Delta \varphi - \varphi \Delta G^{3/2} = 12\mu \left( \frac{\partial G}{\partial t} + \frac{1}{P_0} \frac{\partial G^{-1/2} \varphi}{\partial t} \right). \quad (6)$$

Dividing by  $G^{3/2}$  yields:

$$\Delta \varphi - \varphi \frac{\Delta G^{3/2}}{G^{3/2}} = \frac{12\mu}{G^{3/2}} \left( \frac{\partial G}{\partial t} + \frac{1}{P_0} \frac{\partial G^{-1/2} \varphi}{\partial t} \right). \quad (7)$$

The spatial differential operator appearing in (7) is the Laplacian, the eigenmodes of which do not depend on time. Thus, (7) is amenable to classical methods of reduced-order modelling, such as Fourier's method (i.e. modal analysis).

### 2.2 Modal analysis of the transformed Reynolds equation

One looks for a solution of (7) in the form:

$$\varphi(x, y, t) = \sum_{k=1}^N s_k(t) \varphi_k(x, y), \quad (8)$$

With

$$\Delta \varphi_k = -\lambda_k^2 \varphi_k, \quad (9)$$

And

$$\varphi_k(M) = 0, M \in \partial\Omega. \quad (10)$$

Finding these functions is a fairly routine calculation. For example, for a rectangular domain:

$$\begin{aligned} \varphi_k(x, y) &= \phi_{k_1, k_2}(x, y) = A_{k_1, k_2} \sin\left(k_1 \frac{\pi}{L} x\right) \sin\left(k_2 \frac{\pi}{W} y\right) \\ \{x, y\} &\in [0, L] \times [0, W] \end{aligned} \quad (11)$$

where  $A_{k_1, k_2}$  can be chosen so that the modes verify the orthonormality property:

$$\iint_{\Omega} \varphi_k \varphi_l d\Omega = \delta_{kl}. \quad (12)$$

For complex geometries, the mode shapes may be found using finite element analysis, for example.

Now, the right-hand side of (7) can be expanded to:

$$\frac{12\mu}{G^{3/2}} \left( 1 + \frac{3p}{2P_0} \right) \frac{\partial G}{\partial t} + \frac{12\mu}{P_0} \frac{\partial G^{-2} \varphi}{\partial t}. \quad (13)$$

Since only small pressure variations are considered, (7) simplifies to:

$$\Delta\varphi - \varphi \frac{\Delta G^{3/2}}{G^{3/2}} = 12\mu \left( -2 \frac{\partial G^{-1/2}}{\partial t} + \frac{1}{P_0} \frac{\partial G^{-2}\varphi}{\partial t} \right) \quad (14)$$

Assuming (8-10), and projecting on  $\varphi_l$ , (14) becomes:

$$\begin{aligned} & -\frac{P_0}{12\mu} \sum_{k=1}^N s_k \left( \lambda_k^2 \delta_{kl} + \iint_{\Omega} \frac{\Delta G^{3/2}}{G^{3/2}} \varphi_k \varphi_l d\Omega \right) = \\ & -2P_0 \iint_{\Omega} \varphi_l \frac{\partial G^{1/2}}{\partial t} d\Omega + \frac{d}{dt} \left( \sum_{k=1}^N s_k \iint_{\Omega} G^{-2} \varphi_k \varphi_l d\Omega \right) \end{aligned} \quad (15)$$

A reduced model for the squeezed-film damping of a flexible structure assuming large displacements and small pressure variations is thus:

$$\frac{d}{dt}(\mathbf{A}\mathbf{s}) = \frac{d}{dt}\mathbf{f} + \mathbf{H}\mathbf{s}, \quad (16)$$

With

$$f_l = 2P_0 \iint_{\Omega} \varphi_l G^{-1/2} d\Omega, \quad (17)$$

$$H_{kl} = -\frac{P_0}{12\mu} \left( \lambda_k^2 \delta_{kl} + \iint_{\Omega} \frac{\Delta G^{3/2}}{G^{3/2}} \varphi_k \varphi_l d\Omega \right), \quad (18)$$

$$A_{kl} = \iint_{\Omega} G^{-2} \varphi_k \varphi_l d\Omega. \quad (19)$$

One may also rewrite (16) by letting  $\mathbf{u} = \mathbf{A}\mathbf{s} - \mathbf{f}$ :

$$\frac{d\mathbf{u}}{dt} = \mathbf{H}\mathbf{A}^{-1}(\mathbf{u} + \mathbf{f}). \quad (20)$$

Matrices  $\mathbf{H}$  and  $\mathbf{A}$  and vector  $\mathbf{f}$  may be calculated or approximated once and for all for a given structure as a function of, say, the mechanical modes.

### 3 RESULTS

We demonstrate the validity of the reduced-order model by comparing its results to those of a finite difference model of (3) for the forced excitation of a beam. Let us consider a beam clamped at both ends, with length  $L=500 \mu\text{m}$ , width  $W=50 \mu\text{m}$  and gap  $G_0=3 \mu\text{m}$ . For a rectangular domain, the eigenmodes of the Laplacian are given by (10). We force the displacement of the beam at frequency  $f=3 \text{ kHz}$  with an amplitude of  $\alpha G_0$ , i.e.:

$$G(x,t) = G_0(1 - \alpha w_1(x) \sin(2\pi f t)), \quad (21)$$

where  $w_1(x)$  is the first mechanical mode of the (linear) Euler-Bernoulli beam. Equation (16) is then solved using an implicit Euler scheme. The same numerical integration scheme is used for the finite difference model. Fig. 2 shows the pressure at the midpoint of the membrane calculated with the finite difference model with a  $50 \times 50$  mesh, a time interval of two periods and 200 time-steps, for  $\alpha = 0.4$ . We see that the maximum pressure variation is on the order of  $P_0/10$ , which corresponds to the limit of validity of both models. We show in Fig. 3, the relative error between the proposed model (using  $2 \times 2$  modes) and the finite difference model for several values of  $\alpha$ . The relative error is defined as the relative quadratic error between the projections of the pressures calculated with both models on  $w_1(x)$ , i.e.

$$\varepsilon(\alpha) = \frac{\| \langle P_{ROM}(\alpha) | w_1 \rangle - \langle P_{FD}(\alpha) | w_1 \rangle \|_2}{\| \langle P_{FD}(\alpha) | w_1 \rangle \|_2}. \quad (22)$$

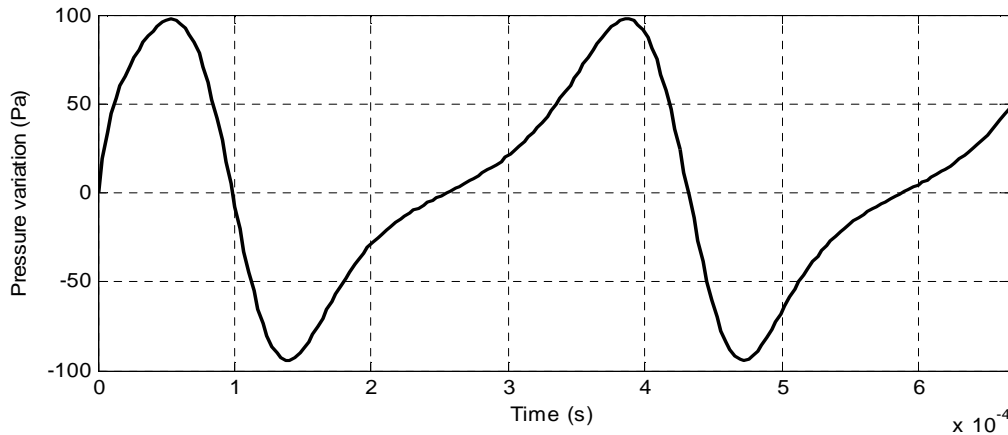


Fig. 2 - Plot of the pressure variation at the midpoint of the membrane for  $\alpha = 0.4$ .

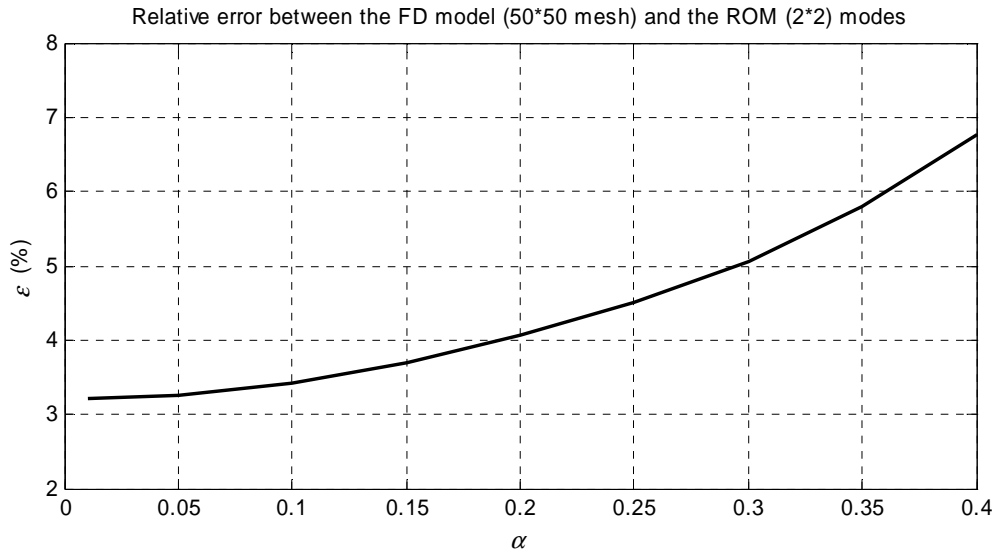


Fig. 3 - Plot of the relative error between the finite difference model and the reduced-order model.

We see that there exists a constant error term of about 3%, even for very small values of  $\alpha$ . This can be reduced by diminishing the step size and by refining the finite difference mesh. As  $\alpha$  increases, the difference between the two models becomes more marked (although it remains quite small). At the limit of validity of the two models, the total relative error is under 7%. The corresponding squeeze number for  $\alpha = 0.4$  is about 100.

#### 4 CONCLUSION

A reduced-order model of the Reynolds equation has been presented. It is valid for large displacements of flexible structures, within the limits of small pressure variations. The accuracy of the model was illustrated by comparing its results with those of a finite difference model. It can then be coupled to a mechanical model so as to extract resonance frequencies and quality factors of microbeam resonators [8] or switching times for electrostatic microswitches, for example. Further work should also concern the extension of the proposed approach to large pressure variations.

#### REFERENCES

[1] M.-H. Bao, "Micro Mechanical Transducers Pressure Sensors, Accelerometers, and Gyroscopes", Amsterdam, Elsevier 2000

- [2] T. Veijola, H. Kuisma, J. Lahdenpera, T. Ryhänen, "Equivalent-circuit model of the squeezed gas film in a silicon accelerometer", *Sensors and Actuators A* 48, pp. 239-248, 1995
- [3] Y. J. Yang, M. A. Gretillat, S. D. Senturia, "Effect of Air Damping on the Dynamics of Non-uniform Deformations of Microstructures", *Transducers'97*, pp.1093-1096, vol. 2, 1997
- [4] M. Younis, A. H. Nayfeh, "Microplate Modeling under Coupled Structural-Fluidic-Electrostatic Forces", *NSTI-Nanotech 2004*, pp. 251-254, vol. 2, 2004
- [5] J. E. Mehner, W. Doetzel, B. Schauwecker, D. Ostergaard, "Reduced order modelling of fluid structural interactions in MEMS based on modal projection techniques", *Transducers'03*, pp 1840-1843 vol. 2, 2003
- [6] E. S. Hung, S. D. Senturia, "Generating Efficient Dynamical Models for Microelectromechanical Systems from a Few Finite Element Simulation Runs", *IEEE Journal of Microelectromechanical Systems*, pp. 280-289, vol. 8, 1999
- [7] M. Rewienski, J. White, "A Trajectory Piecewise-Linear Approach to Model order Reduction and Fast Simulation of Nonlinear Circuit and Micromachined Devices", *IEEE Transactions on CAD of integrated circuit and systems*, pp. 155-170, vol. 22, 2003
- [8] R. Legtenberg, H. A.C. Tilmans, "Electrostatically driven vacuum-encapsulated polysilicon resonators Part I. Design and fabrication", *Sensors and Actuators A*, Vol.45, pp.57-66